JTTEE5 7:50-57

Thermal Spraying of Functionally Graded Calcium Phosphate Coatings for Biomedical Implants

Y. Wang, K.A. Khor, and P. Cheang

(Submitted 25 February 1997; in revised form 14 October 1997)

Biomedical requirements in a prosthesis are often complex and diverse in nature. Biomaterials for implants have to display a wide range of adaptability to suit the various stages of the bio-integration process of any foreign material into the human body. Often, a combination of materials is needed. The preparation of a functionally graded bioceramic coating composed of essentially calcium phosphate compounds is explored. The coating is graded in accordance to adhesive strength, bioactivity, and bioresorbability. The bond coat on the Ti-6Al-4V stub is deposited with a particle range of the hydroxyapatite (HA) that will provide a high adhesive strength and bioactivity but have poor bioresorption properties. The top coat, however, is composed of predominantly α-tricalcium phosphate (α-TCP) that is highly bioresorbable. This arrangement has the propensity of allowing accelerated bio-integration of the coating by the body tissues as the top layer is rapidly resorbed, leaving the more bioactive intermediate layer to facilitate the much needed bioactive properties for proper osteoconduction. The processing steps and problems are highlighted, as well as the results of post-spray heat treatment.

Keywords: α-tricalcium phosphate, calcium phosphates, functionally graded materials (FGM), hydroxyapatite, plasma spraying

1. Introduction

Functionally graded materials (FGM) have a gradient compositional change from the surface to the interior of the material. With the unique microstructure of FGM, material for specific functional and performance requirements can be designed. The potential value of FGMs has attracted much attention in different fields such as aerospace, electrical power generation, and biomaterials (Ref 1-3). In the field of biomaterials, several approaches exist for the deposition of calcium phosphate coatings onto the titanium alloy surfaces (Ref 4-6). Ti-6Al-4V is nontoxic and has low density (4.5 g/mL) and sufficient mechanical strength (tensile strength is ~860 to 895 MPa) (Ref 7). Certain forms of calcium phosphate, such as HA, have good bioactivity and excellent biocompatibility with osseous tissues (Ref 8, 9). The combination of Ti-6Al-4V and calcium phosphate can be applied to work in tandem to produce a biomaterial coating with excellent mechanical and bioactive properties (Ref 10). Among different surfacing processes, thermal spray techniques offer attractive prospects for the economic and efficient deposition of calcium phosphates. Plasma sprayed calcium phosphate coatings have been actively studied, and positive results have been obtained from both in vitro and in vivo tests (Ref 8, 9, 11-14).

Calcium phosphates have different phases. Hydroxyapatite (HA, $Ca_{10}(PO_4)_6(OH)_2$) has excellent chemical bonding ability with natural bone and has been widely studied (Ref 11-14). Tricalcium phosphate (TCP, $Ca_3(PO_4)_2$), known in its two polymorphs of α-TCP and β-TCP, is a bioresorbable ceramic which dissolves gradually in body fluid, and new bone will eventually replace it (Ref 15). The solubility of α-TCP is higher than β-TCP. Harada found that a mixture of α-TCP and HA bonds to bone faster than HA alone (Ref 16). Although the mechanism of bone formation on HA or TCP surfaces and the resorption process of TCP is not yet clearly understood, it is reasonable to say that α-TCP dissolves around HA and provides calcium and phosphate ions which are essential for bone to grow onto the surface of the implant. In vivo testing conducted by Claes et al. showed that the volume of newly formed bone on a TCP surface is higher than that on an HA surface (Ref 17). However, TCP when applied as a thin layer of coating on the surface of implants can totally dissolve over time, thus undesirably exposing the metallic surface to surrounding tissues and fluids.

A functionally graded calcium phosphate coating (Fig. 1) was designed to provide improved bioresorbability for the coating surface. The top layer could provide calcium and phosphate materials for accelerated bone formation. The first layer coated on the titanium substrate is spheroidized HA (SHA) ranging from 20 to 45 μm. Previous studies revealed that using SHA powder can produce a very dense coating structure which might result in higher bond strength with Ti-6Al-4V substrates (Ref 18, 19). TCP/HA composite was deposited in the middle of HA and TCP coatings as a transition layer.

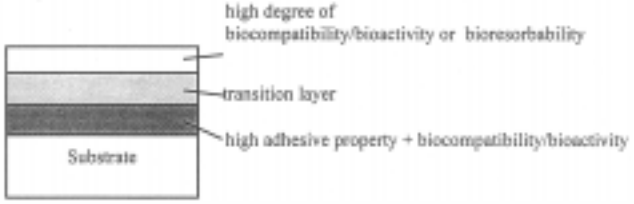

Fig. 1 Schematic illustration of calcium phosphate FGC

Y. Wang, K.A. Khor, and **P. Cheang,** Nanyang Technological University, Singapore 63 9798, Singapore.

2. Experimental Techniques

2.1 *Powder Preparation*

Three types of starting powders were used in this study; that is, calcined HA (CHA) powder supplied by Kyoritsu Ceramic Materials Co. Ltd., Japan; commercial spray dried HA (SDHA, lot No. 16060-004); and calcined α-TCP powder (lot No. 16024-006) obtained from Taihei Chemical Industrial Co. Ltd., Tokyo, Japan.

Calcined HA and ball milled α-TCP were spheroidized by combustion flame spraying (Miller FP73, Wisconsin, USA). The combustion gas mixture was oxygen and acetylene. The flame spheroidized powder was subsequently sieved using a sonic sieve shaker (Fritsch GmbH, Germany). The particle size ranges of HA and α-TCP used for plasma spray were 20 to 45 μm and 1 to 45 μm, respectively.

A spray dryer (LT-8, Ohkawara Kakohki Co. Ltd., Japan) was used to mix the SDHA with ball milled α-TCP powder (approximately 5 to 45 μm), using a binder of 1% polyvinyl alcohol. The debinding process was conducted at 400 °C for 2 h followed by sintering at 800 °C for 2 h. Table 1 shows the parameter of the spray drying process.

2.2 *Plasma Spraying*

Ti-6Al-4V rods and plates were used as the substrates. Prior to plasma spraying, the surfaces of the substrates were grit blasted with silicon carbide grit followed by ultrasonic cleaning in acetone. The surface roughness, R_a, of the substrates was ~3.5 to approximately 4.0 μm. The coatings that were peeled off for the investigation of phase transformation were produced by spraying the powder on the surfaces of aluminum plates. A 40 kW plasma torch (Miller Thermal Inc., Wisconsin, USA) equipped with a computerized closed loop controlled rotor powder feed hopper was used to deposit different layers of coatings on the substrates. The spraying condition is shown in Table 2. After plasma spraying, the peeled off coatings were heat treated in the temperature range of ~600 to 1000 °C for 1 h, and some coatings on Ti-6Al-4V stubs were hot isostatically pressed (HIP) without encapsulation at 900 °C for 3 h under 150 MPa. The HIP equipment used was Kobelco System 5x Series (Kobe, Japan).

Table 1 Spray drying condition

Atomizer	~25 000 to 30 000 rpm
Exhaust air temperature	T_o = 140 °C
Inlet air temperature	T_i = 200 °C
Cyclone pressure	75 to 100 Pa

Table 2 Plasma spraying condition

Main arc gas (argon)	0.28 MPa
Auxiliary gas (helium)	0.28 MPa
Arc current	~800 to 830 A
Arc voltage	~30 to 35 V
Spraying distance	~8 to 10 cm

Table 3 Highest diffraction pattern lines attributed to hkl planes in the calcium phosphates

Phases	Chemical formulation	hkl of the highest peak	2θ°	d-value, Å
HA	$Ca_5(PO_4)_3(OH)$	211	31.7638	2.815
α-TCP	$Ca_3(PO_4)_2$	170	30.7558	2.905
β-TCP	$Ca_3(PO_4)_2$	217	31.0321	2.880
TTCP	$Ca_4O(PO_4)_2$	040	20.8134	2.995
CaO	CaO	200	37.3377	2.406

2.3 *Phase Identification and Morphology Analysis*

A Philips MPD 1880 diffractometer system (Almelo, The Netherlands) was used for phase identification. The operating parameters were CuKα radiation (45 kV/30 mA), divergence slit of 1 degree, receiving slit width of 0.1 mm, a 2θ step scan rate of 1 degree/min and a step size of 0.015 degree. Determination of the phase ratios of HA to TCP (tricalcium phosphate), TTCP (tetracalcium phosphate), and CaO (calcium oxide) phases in the coatings was performed by comparing the integrated area of the most intense peaks of these phases using a profit fitting software in the XRD system. Table 3 lists the highest diffraction pattern lines attributed to the hkl planes in the HA, TCP, TTCP, and CaO phases.

A Cambridge Stereo Scan S360 scanning electron microscope (UK) with an energy dispersive x-ray analyzer (EDX) and a wavelength dispersive x-ray unit (WDX) was used to study the microstructure and Ca/P ratios of both powders and coatings. A Perkin Elmer 7 Series (UNIX TGA 7) thermogravimetric analyzer was used to perform the thermogravimetric analysis (TGA).

2.4 *Mechanical Properties*

The tensile adhesion test (TAT) specified by ASTM C 633-79 was used to measure the tensile bonding strength of the coating. A thin layer of Araldite glue (Ciba-Geigy Ltd., Switzerland) was applied. The tensile fracture strength of the adhesive glue is 22 MPa. After 48 h of curing at ambient atmosphere, the bonding strength was measured using an Instron 4302 tester (10 kN load cell; Boston, MA) at a crosshead speed of 1 mm/min.

3. Results and Discussion

3.1 *Powder Preparation*

After flame spraying, HA particles below 80 μm have been effectively spheroidized (Fig. 2). The relatively low flame temperature (3100 °C) of the combustion spraying limits the melting of large HA particles (Ref 20). On the other hand, the decomposition of HA was also minimized by the low flame temperature. However, the crystallinity of SHA powders becomes progressively lower with decreasing particle size and it can be increased through further heat treatment at 600 to 800 °C prior to plasma spraying (Ref 21). The SHA particles ranging from 20 to 45 μm were used as the feedstock of the first layer of the TCP/HA FGC in this study. The ball milled and sieved α-TCP powder ranging from 1 to 45 μm was also successfully spheroidized (Fig. 3) without significant phase change.

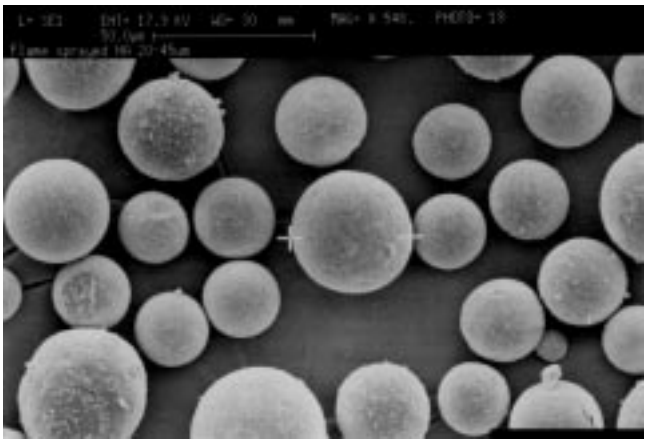

Fig. 2 Spheroidized HA powder by flame spraying (~20 to 45 μm). (Art has been reduced to 69% of its original size for printing.)

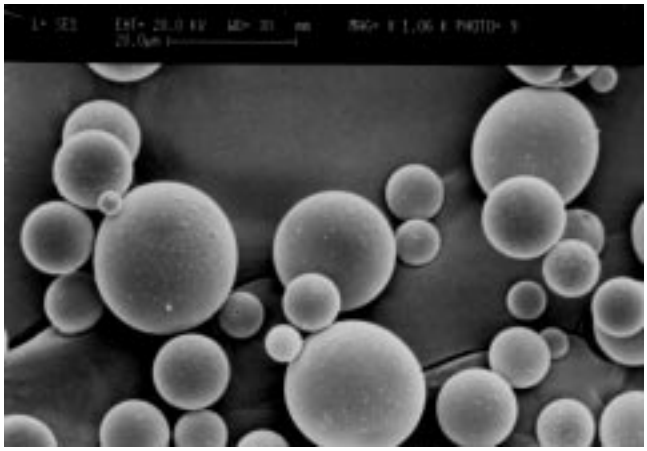

Fig. 3 Spheroidized α-TCP powder by flame spraying. (Art has been reduced to 69% of its original size for printing.)

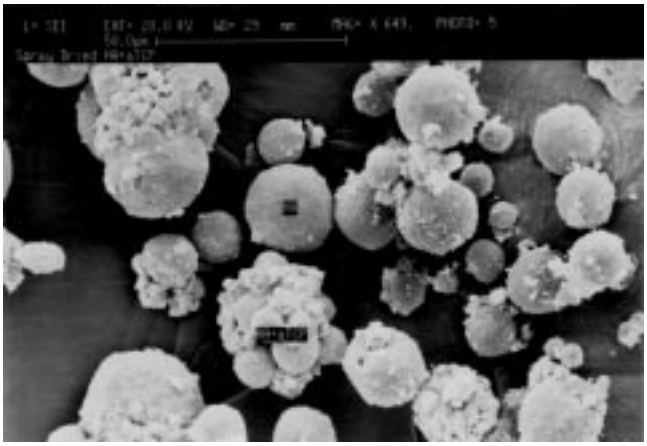

Fig. 4 Spray dried α-TCP/HA powder. (Art has been reduced to 69% of its original size for printing.)

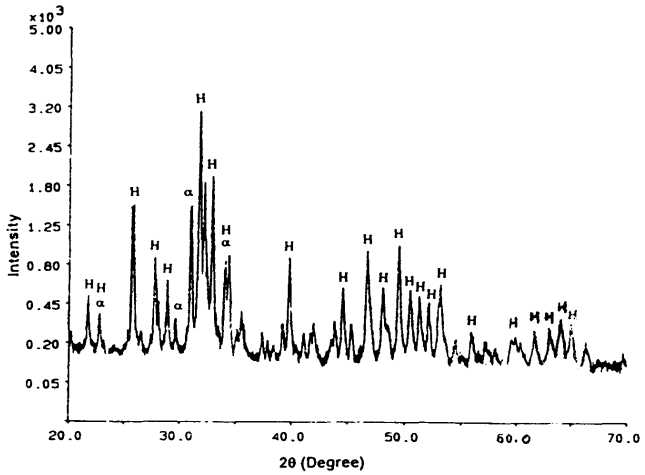

Fig. 5 XRD spectra of spray dried α-TCP/HA powder

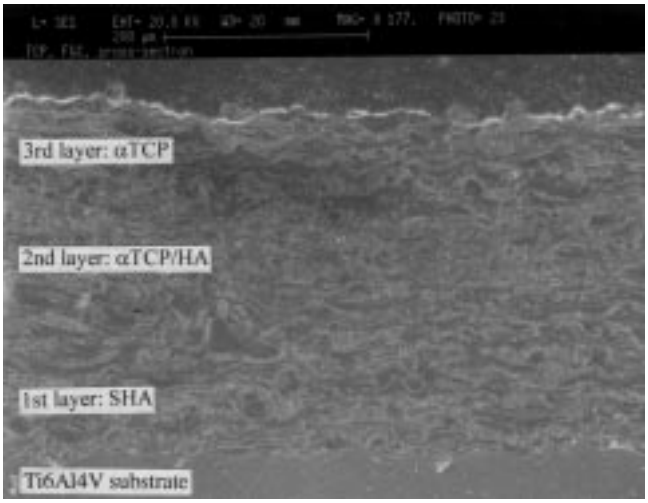

Fig. 6 Cross section view of TCP/HA FGC. (Art has been reduced to 74% of its original size for printing.)

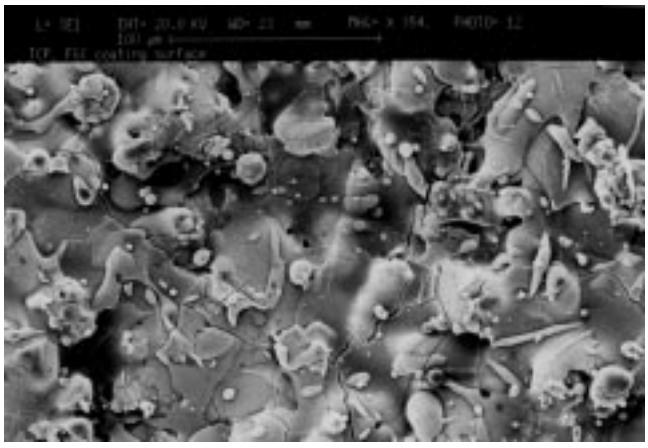

Fig. 7 Surface of TCP/HA FGC. (Art has been reduced to 69% of its original size for printing.)

Particle morphology and XRD spectra of spray dried HA + α-TCP are shown in Fig. 4 and 5, respectively. Small particles are agglomerated to form bigger particles. This powder was significantly porous, and its flowability was inferior to the spheroidized HA and α-TCP.

3.2 *Functionally Graded Coating (FGC)*

3.2.1 Microstructure

The coating cross section (Fig. 6) was relatively dense, consisting of a lamellar structure without obvious boundaries between the layers. The porosity of the second layer deposited by the spray dried TCP/HA powder was slightly higher than that of other layers. This confirmed the earlier investigation on the effect of different feedstocks on the characteristics of HA coatings (Ref 18, 19). The coating surface deposited by spheroidized α-TCP powder reveals well flattened splats with some microcracks (Fig. 7). This coating surface is consistent with the previous report that suggested that HA coatings deposited using spheroidized powder exhibited better quality than that deposited using agglomerated powders, such as calcined and spray dried powders (Ref 19). The cracks are attributed to stresses induced by expansion or contraction of the matrix.

3.2.2 Phase Characterization

Figure 8(a) shows the XRD spectra of the three layers of the as-sprayed FGC. The first layer generated with ~20 to 45 μm SHA powder contained crystalline HA, α-TCP, TTCP, CaO, and amorphous calcium phosphate (ACP) phases. The high decomposition level is due to the small particle size of the feedstock. Small particles could be easily melted during plasma spraying. Conversely, the rapid quenching of the liquid droplets during plasma spraying resulted in formation of amorphous calcium phosphate (ACP) phases. Also, the composition of the hydroxyapatite influences the formation of the amorphous phase. A hydroxyl deficient molten particle will more likely form an

Table 4 Ca/P ratio of raw powders and TCP/HA FGC

	HA raw powder	TCP raw powder	First layer of FGC (~20 to 45 μm SHA)	Second layer of FGC (TCP/HA)	Third layer of FGC (TCP)
Ca/P ratio	1.75	1.50	2.10	2.56	2.00

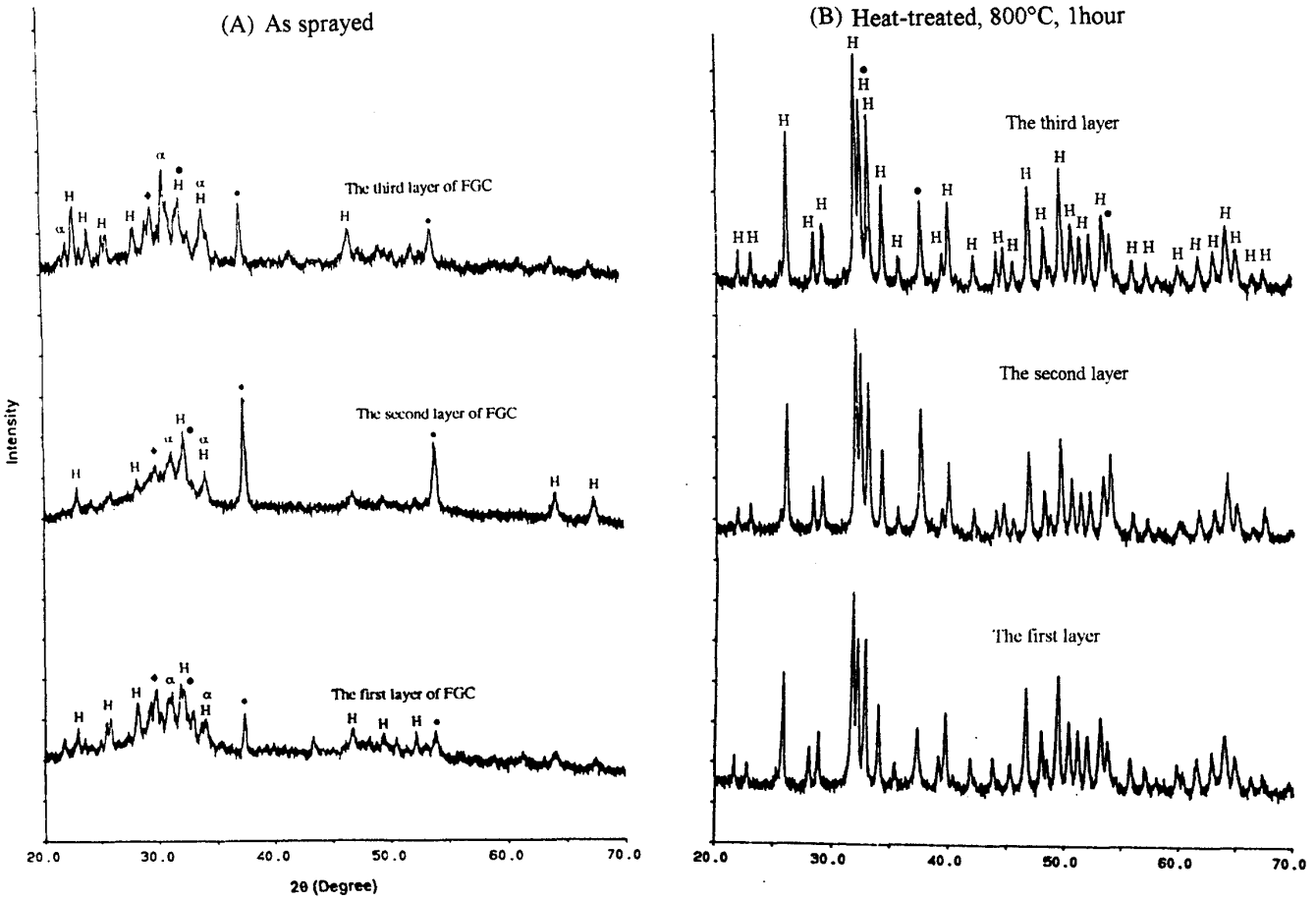

Fig. 8 XRD patterns of as-sprayed and heat-treated α-TCP/HA FGC. H is HA, α is α-TCP; closed diamond is TTCP. Closed circle is CaO.

amorphous phase compared to a droplet with a high hydroxylation level (Ref 22). Therefore, the formation of amorphous phases was a result of rapid cooling of molten droplets, as well as dehydroxylation taking place in the droplets during plasma spraying.

The middle layer is composed predominantly of ACP and CaO. This is due to the weak bonding of the spray dried particles. When the agglomerated powder was injected into the high velocity and high temperature plasma flame, it easily disintegrated. Since the fragmented powder is very small, it will melt completely and the droplets would increase in heat to a high temperature even though the residence time was only several milliseconds. It was reported that when the calcium phosphate ceramic is heated above ~1700 °C, only CaO remains as a solid (Ref 23, 24). When the droplets that consisted of a mixture of liquid calcium phosphate and CaO phase were quenched, the CaO and ACP phases become the main components in the coating. Crystallized TCP and ACP were the primary phases in the top layer which suggests a high bioresorbability. The ACP phase, as mentioned earlier, resulted from the rapid solidification of the melted particles.

WDX results show that the Ca/P ratios of the three layers of α-TCP/HA FGC changed during plasma spraying (Table 4). The more extensive the decomposition, the higher the Ca/P ratio. Therefore, as a result of the extremely high temperature of the plasma flame, not only the OH group, but also some P_2O_5 were lost (Ref 25). Since the particle size and morphology determine the melting behavior of the feedstock and affect the coating structure and phase composition, it can be deduced that the Ca/P ratios were also affected by the same factors.

3.2.3 Heat Treatment of Coatings

After heat treatment at 800 °C for 1 h, the XRD patterns of the individual TCP/HA FGC layers show a highly crystallined HA phase (Fig. 8b), the TTCP phase was no longer detected by XRD analysis, and only a trace of TCP phase was detected. However, the CaO phase still remained. The transformation of TCP and TTCP to HA was found on the surface of TCP cement when it was immersed in water or body fluids as Eq 1 and 2 indicate (Ref 26). In such a case, TCP and TTCP were called " defective apatite" (Ref 27). The TCP and TTCP phases, as decomposition products in HA plasma sprayed coating, were also reported to have converted back to HA during post-spray heat treatment according to the XRD patterns (Ref 28).

$$4Ca_3(PO_4)_2(s) \rightarrow Ca_{10}(PO_4)_6(OH)_2(s) + 2Ca^{2+} + 2HPO_4^- \quad \text{(Eq 1)}$$

$$3Ca_3(PO_4)_2(s) + 3H_2O \rightarrow Ca_{10}(PO_4)_6(OH)_2(s) + 2Ca^{2+} + 4OH^- \quad \text{(Eq 2)}$$

In order to study the phase transformation in powders and coatings during heat treatment, TCP, TCP/HA powders, and peeled off coatings were heat treated under different tempera-

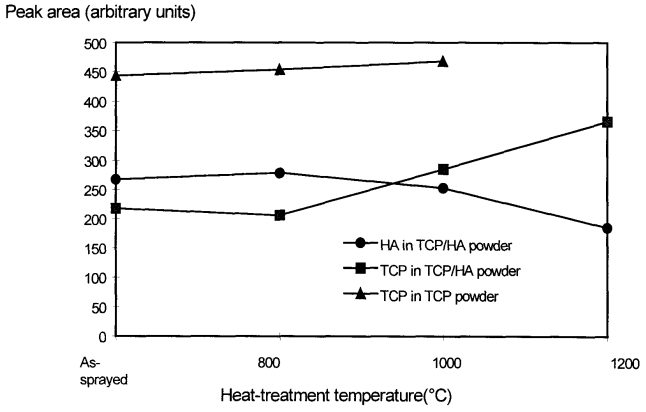

Fig. 9 Peak area of TCP(α + β) and HA phases in TCP/HA and TCP powders post heat treatment

Table 5 Phase ratios of the as-sprayed and heat-treated TCP/HA and TCP coatings

	TCP/HA	TTCP/HA	CaO/HA
TCP/HA coating	1.48	0.13	1.05
600 °C	0.04	0	0.16
800 °C	0.01	0	0.21
1000 °C	0	0	0.32
α-TCP coating	7.04	1.68	1.92
600 °C	0.16	0	1.68
800 °C	0.03	0	0.84
1000 °C	0	0	0.22

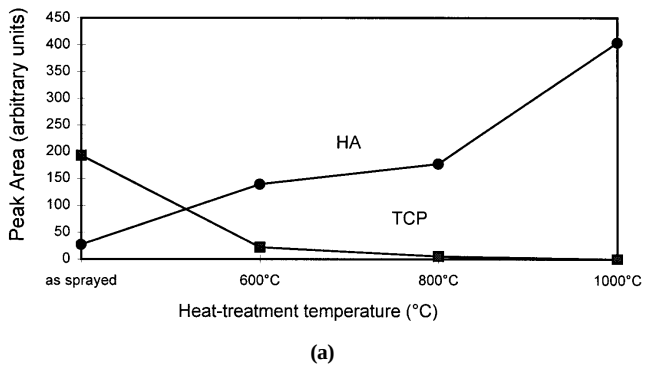

(a)

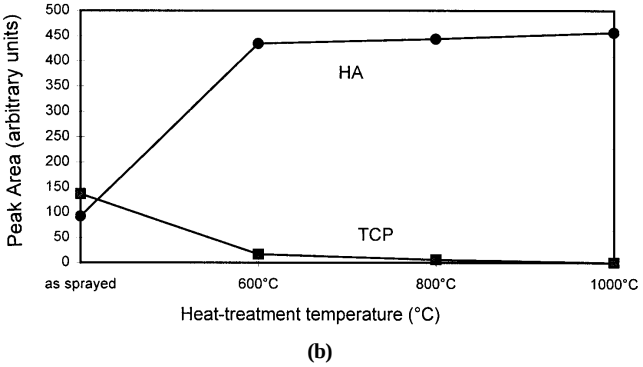

(b)

Fig. 10 Peak area of TCP(α + β) and HA phases in as-sprayed and heat-treated **(a)** TCP/HA coatings and **(b)** TCP coatings

tures. After heat treatment at 800 and 1000 °C for 1 h, no phase change was detected in the TCP powder. After heat treatment at 1200 °C, some α-TCP transformed to β-TCP. This is because a high temperature stable α-TCP phase (stable temperature range is 700 to 1200 °C) (Ref 26) transformed to β-TCP during furnace cooling. As for the TCP/HA powder, heat treatment higher than 1000 °C caused HA to decompose, and the amount of TCP (α-TCP and β-TCP) phases increased. Figure 9 shows the peak area of TCP (α + β) and HA phases in TCP/HA powder and TCP powders after heat treatment.

The heat treatment results show that the TCP phase in both TCP and TCP/HA powders did not convert to HA during heat treatment. However, when TCP/HA and TCP coatings were heat treated under 600, 800, and 1000 °C, the TCP peak area decreased with increasing heat treatment temperature. Meanwhile, the HA peak area increased correspondingly (Fig. 10). Table 5 shows the change in the phase ratios of the as-sprayed and heat treated TCP/HA and TCP coatings. The heat treatment resulted in apparent conversion of the TCP, TTCP, and amorphous calcium phosphate phases to crystalline HA. The CaO/HA ratio in the heat-treated HA/TCP coating increased with the heat treatment temperature, although these CaO/HA ratios were smaller than that in the as-sprayed coating. This is consistent with the observation of HA coatings in the previous work (Ref 29). The increase in the CaO/HA ratio suggests that heat treatment could result in decomposition of certain unstable calcium phosphate phases to predominantly CaO due to the high Ca/P ratio in this coating (Table 4.) However, the CaO/HA ratio in the heat-treated TCP coating decreased with the heat-treatment temperature.

In the plasma sprayed HA coatings, TCP phase is the decomposition product of HA, and the TCP phase in the TCP/HA coating came from both the TCP feedstock and the decomposition of HA. The equilibrium phase diagram of $CaO\text{-}P_2O_5\text{-}H_2O$ shows that HA decomposed at a high temperature that depends on the partial pressure of H_2O (Eq 3 and 4), and these reactions are reversible (Ref 27, 30). The temperature ranges from 1325 to 1550 °C in the presence of water (partial pressure from 6.7×10^2 to 1.33×10^4 Pa).

$$Ca_{10}(PO_4)_6(OH)_2(HA) \leftrightarrow 2Ca_3(PO_4)_2(TCP) + Ca_4P_2O_9(TTCP) + H_2O \uparrow \quad \text{(Eq 3)}$$

$$2Ca_{10}(PO_4)_6(OH)_2(HA) \leftrightarrow 3Ca_3(PO_4)_2(TCP) + CaO + H_2O \uparrow \quad \text{(Eq 4)}$$

The Ca/P ratio is an important quantity for calcium phosphate ceramics, and this changed during the plasma spraying process (Ref 25, 26, 31, 32). As a result, CaO precipitated from the liquid calcium phosphate. With the precipitation of CaO, the Ca/P ratio decreased. Within a certain range of Ca/P ratio, the stable phase of calcium phosphate will be essentially HA up to 1200 to 1300 °C from a crystallographic viewpoint (Ref 27). The Ca/P ratio range within which the HA is stable is affected significantly by the partial pressure of water (Ref 31). TGA results (Fig. 11) show that there is an increase in weight (~5.5%) of TCP coating during post-spraying heat treatment. It seems that the conversion of TCP and TTCP to HA is the reverse of Eq 3 and 4. The decrease in CaO/HA ratio in the heat-treated TCP coating (Table 5) also suggested the possibility of the reversion of Eq 4. However, the analysis based on the XRD result is limited because the difference between the XRD patterns of the vacancy state and stoichiometric HA is not obvious. It is also difficult to distinguish the phase transformation mechanism in HA coating and TCP coating only by XRD analysis.

The heat-treatment results show that the heat-treated FGC was no longer an FGC as in the as-sprayed state. All layers of the previous FGC showed similar XRD patterns except in the difference of CaO amount. Although post-spray heat treatment improved the crystallinity of HA coatings, it seems that in the TCP/HA FGC system, heat treatment did not provide any additional advantage to the coating. The as-sprayed coatings should be used directly to test the bioactivity and biocompatibility of this FGC system.

3.3 *Bond Test*

The average coating thickness of the FGC is 220 μm. The bond strength of the as-sprayed coating and hot isostatic pressed coating (at 900 °C for 3 h) was 6.67 MPa and 6.62 MPa, respectively. The fracture of all specimens occurred at the interface between coatings and substrates and suggests that the adhesive bond strength of these coatings was lower than the cohesive bond strength between different layers. It is reported that the HA coating would react with titanium substrate during heat treatment to generate some chemical bonding at the interface (Ref 33). Theoretically, the bond strength should be higher after hot isostatic pressing. However, when the cooling rate of the hot isostatic pressing was too fast, the difference of the thermal expansion coefficients between the coating and the substrate became the main factor for the reduced bond strength.

Another way to improve the adhesive tensile bond strength of calcium phosphate coatings is to reduce overall coating thickness. Previously, it was shown that the tensile bond strength could be improved considerably when the overall coating thickness was decreased approximately 60 to 80 μm (Ref 29).

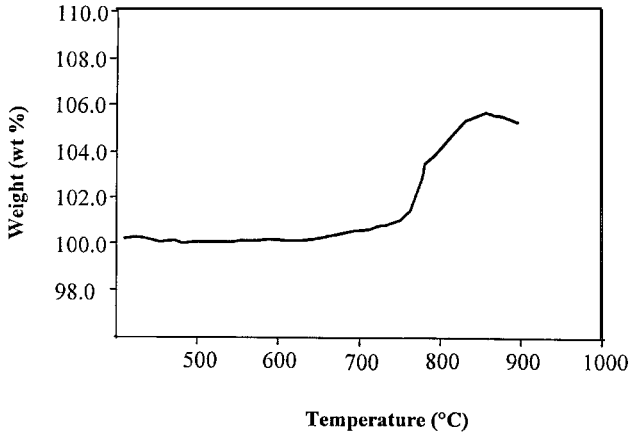

Fig. 11 TGA test results of α-TCP coating

4. Conclusions

Functionally graded calcium phosphate coatings were produced on Ti-6Al-4V substrates by plasma spraying. The microstructure of the coating was dense and showed the typical plasma sprayed lamellar structure. The top layer of the coating was mainly composed of α-TCP which suggests high bioresorbability. However, after post-spray heat treatment, the TCP phase, from either the decomposition of HA or the TCP feedstock, and the TTCP phase were no longer detected by XRD, while the CaO phase still remained. The loss of the OH group and P_2O_5 occurred during plasma spraying. The phase composition after post-sprayed heat treatment was affected by the change in the Ca/P ratio. Nevertheless, an appropriate powder processing procedure and combinations of calcium phosphates can yield coatings with varying amounts of crystalline HA and α-TCP. Both are found to be beneficial to accelerated osseo-induction properties. The prevention of CaO formation in the coating remains to be attained. The cohesive strength between different layers of the coating was found to be stronger than the adhesive strength between the coating and substrate.

5. Acknowledgments

Financial support for the plasma spray from NTU RP 56/92 and JT ARC 4/96 is gratefully acknowledged. The technical assistance provided by Mr. Lim Kok Yong and Mdm. Yong Mei Yoke is gratefully acknowledged.

References

1. M. Koizumi and M. Niino, Overview of FGM Research in Japan, *MRS Bulletin*, Jan 1995, p 19-21
2. M. Kawamura, Y.M.J. Fujioka, S. Yamazaki, S. Nishio, E. Tada, and T. Abe, Fabrication of Functionally Gradient Materials for Electric Insulation of Fusion Reactor Components, Advanced Materials '93, III/B, *Trans. Mater. Research Society,* M. Sakai, M. Kobayashi, T. Suga, R. Watanabe, Y. Ishida, and K. Niihara, Ed., 16B, Materials Research Society, 1994, p 1251-1254
3. S.W. Huelsman and W.G.J. Bunk, Fabrication of Graded Metal-Ceramic Material by Powder Technology and Its Thermo-Mechanical Evaluation, Advanced Materials '93, III/B, *Trans. Mater. Research Society,* M. Sakai, M. Kobayashi, T. Suga, R. Watanabe, Y. Ishida, and K. Niihara, Ed., 16B, 1994, p 1259-1262
4. C.P.A.T. Klein, J.G.C. Wolke, J.M.A. de Blieck-Hogervorst, and K. de Groot, Calcium Phosphate Plasma-Sprayed Coatings and Their Stability: An In Vivo Study, *J. Biomed. Mater. Res.*, Vol 28, 1994, p 909-917
5. B.C. Wang, E. Chang, and C.Y. Yang, A Histomorphometric Study on Osteoconduction and Osseointegration of Titanium Alloy with and without Plasma-Sprayed Hydroxyapatite Coating Using Back-Scattered Electron Images, *J. Mater. Sci.: Mater. Med.*, Vol 4, 1993, p 394-423
6. S.L. Evans, K.R. Lawes, and P.J. Gregson, Layered, Adhesively Bonded Hydroxyapatite Coatings for Orthopedic Implants, *J. Mater. Sci.: Mater. ed.*, Vol 5, 1994, p 495-499
7. J.B. Park, *Biomaterials Science and Engineering*, Plenum Press, 1984, p 212-216
8. S.D. Cook, K.A. Thommas, J.E. Dalton, T.K. Volkman, T.S. Whitecloud III, and J.F. Kay, Hydroxyapatite Coating of Porous Implants Improves Bone Ingrowth and Interface Attachment Strength, *J. Biomed. Mater. Res.*, Vol 26, 1992, p 989-1001
9. K. de Groot, R. Geesink, C.P.A.T. Klein, and P. Serekian, Plasma Sprayed Coatings of Hydroxyapatite, *J. Biomed. Mater. Res.*, Vol 21 (No. 12), 1988, p 1375-1381
10. P. Ducheyne, S. Radin, M. Heughebaert, and J.C. Heughebaert, Calcium Phosphate Ceramic Coatings on Porous Titanium: Effect of Structure and Composition on Electrophoretic Deposition, Vacuum Sintering and in vitro Dissolution, *Biomaterials*, Vol 11, 1990, p 244-254
11. C.L. Tisdel, V.M. Goldberg, J.A. Parr, J.S. Bensusan, L.S. Staikoff, and S.S. Cleveland, The Influence of a Hydroxyapatite and Tricalcium-Phosphate Coating on Bone Growth into Titanium Fiber-Metal Implants, *J. Bone and Joint Surg.*, Vol 76-A (No. 2), 1994, p 159-171
12. H. Oonishi, Orthopedic Applications of Hydroxyapatite, *Biomaterials*, Vol 12, 1991, p 171-178
13. P. Ducheyne, L.L. Hench, A. Kagan, M. Martens, A. Burssens, and J.C. Mulier, The Effect of Hydroxyapatite Impregnation on Skeletal Bonding of Porous Coated Implants, *J. Biomed. Mater. Res.*, Vol 14, 1980, p 225-237
14. R.G.T. Geesink, K. de Groot, and C.P.A.T. Klein, Bone Bonding to Apatite Coated Implants, *J. Bone Joint Surg.*, Vol 70B, 1988, p 17-22
15. L.L. Hench, Bioceramics: From Concept to Clinic, *J. Am. Ceram. Soc.*, Vol 74, 1991, p 1487-1510
16. Y. Harada, Experimental Studies of Healing Process on Compound Blocks of Hydroxyapatite Particles and Tricalcium Phosphate Powder Implantation in Rabbit Mandible, *J. Tokyo Dental College Soc.*, Vol 89, 1989, p 263-297
17. L. Claes, H.J. Wilke, H. Kiefer, and A. Meschenmoser, Bone Effect Bridging with Different Implant Materials, *Handbook of Bioactive Ceramics, Vol 2, Calcium Phosphate and Hydroxyapatite Ceramics*, T. Yamamuro, L.L. Hench, and J. Wilson, Ed., 1990, CRC Press Inc., p 77-86
18. K.A. Khor and P. Cheang, Thermal Spray Industrial Applications, *Influence of Powder Characteristics on Plasma Sprayed Hydroxyapatite Coatings*, C.C. Berndt and S. Sampath, Ed., ASM International, 1994, p 147-152
19. P. Cheang and K.A. Khor, Addressing Processing Problems Associated with Plasma Spraying of Hydroxyapatite Coating, *Biomaterials*, Vol 17, 1996, p 537-544
20. Operator's Manual, Miller Thermal, Inc., Appleton, WI, 1993
21. K.A. Khor and P. Cheang, Plasma Sprayed Hydroxyapatite (HA) Coatings Produced with Flame Spheroidised Powders, *J. Mater. Process. Technol.*, Vol 63, 1997, p 271-276
22. K.A. Gross and C.C. Berndt, The Amorphous Phase in Plasma Sprayed Hydroxyapatite Coatings, Bioceramic, Vol 8, *Proc. Eighth International Symposium on Ceramics in Medicine*, 1995, p 361-366
23. Z. Zyman, Y. Cao, and X. Zhang, Periodic Crystallization Effect in the Surface Layers of Coatings during Plasma Spraying of Hydroxyapatite, *Biomaterials*, Vol 14 (No. 15), 1993, p 1140-1144
24. T. Kijima and M. Tsutsumi, Preparation and Thermal Properties of Dense Polycrystalline Oxyhydroxyapatite, *J. Am. Ceram. Soc.*, Vol 62, 1979, p 455
25. R. McPherson, N. Gane, and T.J. Bastow, Structural Characterization of Plasma-Sprayed Hydroxyapatite Coatings, *J. Mater. Sci.: Mater. Med.*, Vol 6, 1995, p 327-334
26. K. de Groot, C.P.A.T. Klein, J.G.C. Wolke, and J.M.A. de Blieck-Hogervorst, *Chemistry of Calcium Phosphate Bioceramics, Handbook of Bioactive Ceramics*, Vol 2, *Calcium Phosphate and Hydroxyapatite Ceramics*, T. Yamamuro, L.L. Hench, and J. Wilson, Ed., 1990, CRC Press Inc., p 3-15
27. A. Ravaglioli and A. Krajewski, *Bioceramics: Materials, Properties, Applications*, Chapman & Hall, 1992, p 176-185

28. C.C. Berndt and K.A. Gross, Characteristics of Hydroxyapatite Bio-Coatings, *Thermal Spray: International Advances in Coatings Technology*, C.C. Berndt, Ed., ASM International, 1992, p 465-470
29. K.A. Khor, P. Cheang, and Y. Wang, Plasma Spraying of Combustion Flame Spheroidized Hydroxyapatite (HA) Powders, *J. Therm. Spray Technol.*, ASM International, 1997 (in press)
30. C. Rey, M. Freche et al., Apatite Chemistry in Biomaterial Preparation, Shaping, and Biological Behavior, *Bioceramics*, W. Bonfield et al., Ed., Oxford, 1991, p 57-64
31. K. Yamashita, T. Arashi, K. Kitagaki, S. Yamada, T. Umegaki, and K. Ogawa, Preparation of Apatite Thin Films through Rf-Sputtering from Calcium Phosphate Glasses, *J. Am. Ceram. Soc.*, Vol 77 (No. 9), 1994, p 2401-2407
32. P.W. Brown, Phase Relationship in the Ternary System CaO-P_2O_5-H_2O at 25 °C, *J. Am. Ceram. Soc.*, Vol 75 (No. 1), 1992, p 17-22
33. H. Ji, C.B. Ponton, and P.M. Marquis, Microstructure Characterization of Hydroxyapatite Coating on Titanium, *J. Mater. Sci.: Mater. Med.*, Vol 3, 1992, p 283-287